

1 **MODELING THE EFFECTS OF CONGESTION ON FUEL**
2 **ECONOMY FOR ADVANCED POWERTRAIN VEHICLES**

3
4 Alexander Bigazzi
5 Department of Civil and Environmental Engineering
6 Portland State University
7 P.O. Box 751, Portland, OR 97207-0751
8 abigazzi@pdx.edu
9 503-725-4282

10
11 Kelly Clifton
12 Department of Civil & Environmental Engineering
13 Portland State University
14 P.O. Box 751, Portland, OR 97207-0751
15 kclifton@pdx.edu

16
17 Brian Gregor
18 Transportation Planning Analysis Unit
19 Oregon Department of Transportation
20 555 13th Street NE, Suite 2, Salem, OR 97301-4178
21 Brian.J.Gregor@odot.state.or.us

22
23
24
25 Submitted to the 91st Annual Meeting of the Transportation Research Board, January 2012,
26 Washington, D.C.

27
28
29 Original Submission: July 2011
30 Revised: November 2011

31
32
33 7,377 words [5,377 + 2 table x250 + 6 figures x250]
34

35 **ABSTRACT**

36 This paper describes research undertaken to establish plausible fuel-speed curves (FSC) for
37 hypothetical advanced powertrain vehicles. These FSC are needed to account for the effects of
38 congestion in long-term transportation scenario analysis considering fuel consumption and
39 emissions. We use the PERE fuel consumption model with real-world driving schedules and a
40 range of vehicle characteristics to estimate fuel economy (FE) in varying traffic conditions for
41 light-duty internal combustion engine (ICE) vehicles, hybrid gas-electric vehicles (HEV), fully
42 electric vehicles (EV), and fuel cell vehicles (FCV). FSC are fit to model results for each of 145
43 hypothetical vehicles. Analysis of the FSC shows that advanced powertrain vehicles are expected
44 to perform proportionally better in congestion than ICE vehicles (when compared to their
45 performance in free-flow conditions). HEV are less sensitive to average speed than ICE vehicles,
46 and tend to maintain their free-flow FE down to 20 mph. FE increases for EV and FCV from
47 free-flow conditions down to about 20-30 mph. Beyond powertrain type differences, relative FE
48 in congestion is expected to improve for vehicles with less weight, smaller engines, higher
49 hybrid thresholds, and lower accessory loads (such as air conditioning usage). Relative FE in
50 congestion also improves for vehicle characteristics that disproportionately reduce efficiency at
51 higher speeds, such as higher aerodynamic drag and rolling resistance. In order to implement
52 these FSC for scenario analysis, we propose a bounded approach based on a qualitative
53 characterization of the future vehicle fleet. The results presented in this paper will assist analysis
54 of the roles that vehicle technology and congestion mitigation can play in reducing fuel
55 consumption and emissions from roadway travel.

56

57 **1 Introduction**

58 Traffic congestion has been steadily increasing in the U.S. for decades [1]. Increasing levels of
59 congestion lead to longer travel times, lower average speeds, and increased vehicle speed
60 variability. These affect engine/motor operating loads and operating duration, which in turn
61 affect fuel efficiency. At the same time, the U.S. vehicle fleet continues to evolve, with new
62 powertrain types such as Hybrid Electric Vehicles (HEV), Fuel Cell Vehicles (FCV), and fully
63 Electric Vehicles (EV) [2]. This paper addresses how these new vehicle technologies will
64 respond to congestion, in terms of fuel efficiency. The Oregon Department of Transportation
65 (ODOT) has developed a model to forecast transportation-related greenhouse gas emissions,
66 called the Greenhouse gas Statewide Transportation Emissions Planning model or GreenSTEP
67 [3]. GreenSTEP is a modeling tool that can be used to assess the impact of a range of policies
68 and other factors on transportation-related greenhouse gas emissions. It is designed to operate
69 within the context of the large uncertainties of long-term transportation planning. One of the
70 improvements needed in the model is the ability to account for the impact of future technological
71 changes on vehicle fuel efficiency in congestion.

72 Vehicle fuel efficiency can be expressed as Fuel Economy (FE), in travel distance per
73 unit volume of fuel – in the U.S. as miles per gallon (mpg). Fuel-Speed Curves (FSC) summarize

74 the relationship between vehicle fuel economy and congestion level (indicated by travel speed)
75 for average, aggregate conditions. Thus FSC can serve to estimate fuel consumption in
76 congestion for macroscopic traffic and transportation models.

77 In the GreenSTEP model, normalized FSC are used to adjust average fuel efficiencies for
78 varying levels of metropolitan congestion. While FSC for conventional, Internal Combustion
79 Engine (ICE) vehicles have been previously studied (and adopted in GreenSTEP), FSC for
80 advanced powertrain vehicles have received less attention. In order to enable incorporation of the
81 impacts of congestion on advanced vehicles in GreenSTEP, this research develops FSC for HEV,
82 FCV, and EV. Fuel economy at varying average travel speeds is estimated using an advanced-
83 vehicle fuel consumption model with archetypal speed profiles. Then, representative FSC are
84 estimated for each vehicle type, based on a range of vehicle characteristics. The next section
85 describes relevant background information and literature, and is followed by a presentation of the
86 modeling methodology. Then, results for FSC calculation are show, followed by a section
87 discussing of the application of these FSC for transportation scenario analysis.

88 **2 Background and Literature**

89 **2.1 Congestion and Fuel Economy**

90 Traffic congestion affects vehicle fuel economy through lower average travel speed and
91 increased vehicle speed variability (accelerations and decelerations). These influence
92 engine/motor operating loads and operating duration, which in turn impact fuel consumption per
93 mile of travel [4]. FSC show these aggregate relationships as the expected average FE at a given
94 average travel speed, including typical acceleration and deceleration activity (often for specific
95 vehicle and roadway types). In this way the speed variable in FSC is a proxy for congestion
96 level, indicative of both average speed and speed variability for archetypal conditions.

97 FSC are the fuel equivalent of Emissions-Speed Curves (ESC), which are used to
98 estimate the aggregate impact of congestion on vehicle pollution emissions rates [5–7]. The ESC
99 approach has been shown to adequately represent congestion effects (related to both average
100 speed and speed variability) if the curves are based on representative, real-world driving patterns
101 [8], [9]. The EPA has created a set of realistic driving schedules (driving patterns) for inclusion
102 in their MOVES 2010 mobile-source emissions model [10], [11]. Existing research on FSC for
103 ICE vehicles indicates that increasing levels of congestion – with lower average speeds –
104 generally lead to increased fuel consumption rates [6]. At very high speeds, however, fuel
105 consumption rates increase as well, and there is an optimal average speed for fuel economy
106 which depends on the vehicle fleet – typically between 45 and 65 mph [12].

107 **2.2 Fuel Economy of Advanced Vehicles**

108 Given concerns about energy consumption and climate impacts of the U.S. vehicle fleet,
109 there has been considerable attention paid to the potential fuel economy of advanced powertrain
110 vehicles [2], [4], [13], [14]. Fuel economy estimates for advanced vehicles are challenging
111 because few, if any, dynamometer test data are available. Thus, vehicle fuel consumption

112 modeling is often undertaken to estimate or predict the performance of these vehicles. Various
113 studies have demonstrated or predicted substantial fuel consumption or greenhouse gas
114 emissions savings from the substitution of advanced powertrain vehicles for conventional
115 Internal Combustion Engine (ICE) vehicles in the fleet [2], [15–17].

116 Fuel consumption modeling for advanced vehicles has focused on average overall fuel
117 economy. But speed-based or congestion-based FE estimates are needed to predict the effects of
118 varying congestion levels on the performance of these vehicles. Delorme, Karbowski, & Sharer
119 [18] modeled the speed-dependent fuel consumption rates of select medium and heavy-duty
120 vehicles, including several hybrid versions. They point out the importance of using realistic
121 driving patterns and the challenge of a lack of a standard set of vehicle technical specifications
122 for advanced vehicle modeling. Fontaras, Pistikopoulos, and Samaras [19] modeled two hybrid
123 passenger cars and found lower optimal speeds with respect to fuel consumption for the hybrid
124 cars than for conventional cars (and lower overall fuel consumption rates). While modeling such
125 as this suggests different FSC for advanced vehicles than for ICE vehicles, these studies do not
126 provide the array of FSC needed for scenario testing of a variety of potential advanced vehicles
127 in congestion.

128 Beyond the unique mechanical performance of advanced vehicles, some studies have
129 suggested that advanced vehicles are driven differently. An empirical study by the EPA in
130 Kansas City showed less aggressive driving for HEV than for ICE vehicles [11]. The report
131 acknowledges, however, that there are several other possible explanations besides driver
132 behavior change in response to HEV/ICE vehicle differences. Other possibilities include less
133 power available in the test hybrid vehicles and self-selection of fuel-conscious drivers for hybrid
134 ownership. Alessandrini & Orecchini [20] studied EV operating in Rome and also found less
135 aggressive driving – presumably owing to the limited power of the vehicles.

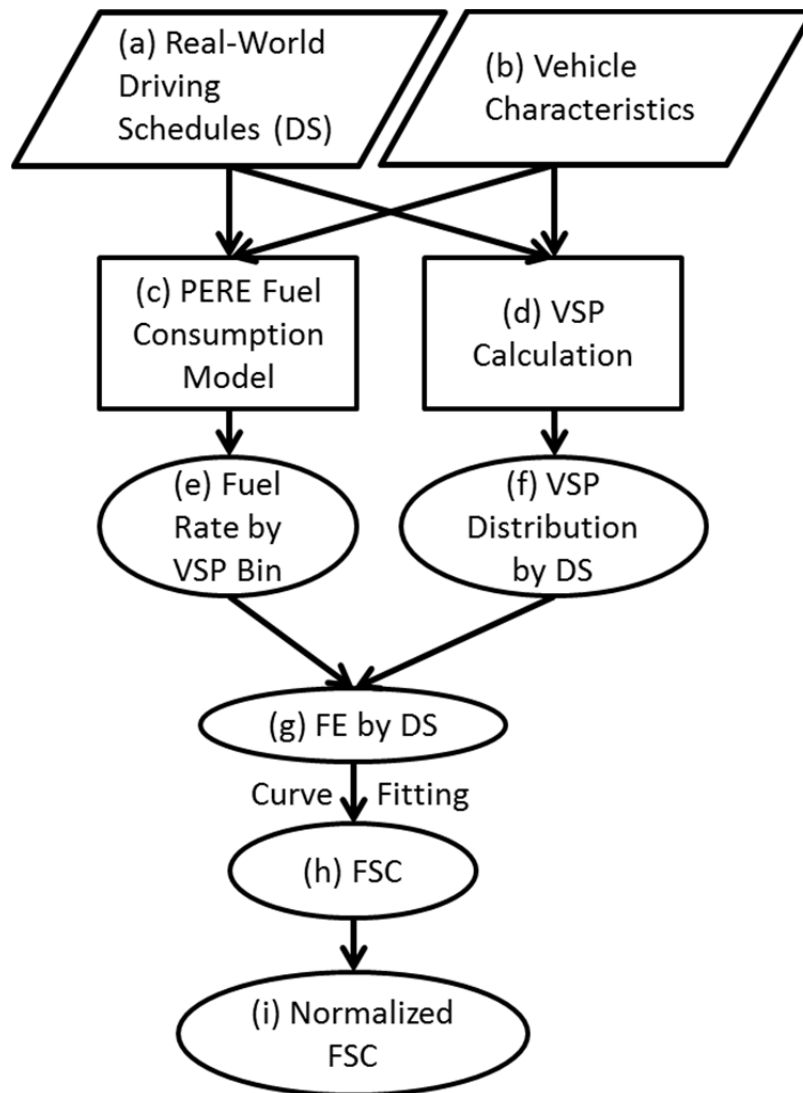
136 **2.3 Modeling Congestion in GreenSTEP**

137 In order to motivate the study methodology, we here describe the role of FSC within
138 GreenSTEP. Average fleet fuel economy by vehicle type and model year is input to each model
139 run. GreenSTEP accounts for congestion effects by adjusting the fleet-average fuel economy (for
140 ICE vehicles only). For each metropolitan area, the Daily Vehicle Miles Traveled (DVMT) are
141 distributed by average speed (average speed ranges are 25-60 mph on freeways and 21-30 mph
142 on arterials). Then, normalized FSC are used to scale the average fleet fuel economy based on
143 the estimated speed distribution of DVMT. Details can be found in the GreenSTEP
144 documentation [3]. The next section describes the modeling methodology of this study, which
145 attempts to develop realistic FE adjustment curves at the GreenSTEP scope of modeling.

146 **3 Methodology**

147 In order to estimate the impacts of congestion on advanced technology vehicles, this
148 research develops FSC for light-duty ICE vehicles, HEV, FCV, and EV. An overview of the
149 modeling procedure is illustrated in Figure 1. First, a large set of real-world driving schedules (a)

150 and a test set of 145 hypothetical vehicles with a variety of characteristics (b) are used as inputs
 151 to the PERE model (c) to estimate fuel consumption rates by Vehicle Specific Power (VSP) bin
 152 (e) for each vehicle. Next, the same set of driving schedules (a) and vehicle characteristics (b) are
 153 used to calculate (d) VSP bin distributions of operating time for each driving schedule, for each
 154 vehicle (f). The driving schedules represent a variety of congestion levels on freeway and arterial
 155 facilities. Combining (e) and (f) generates estimates of average FE for each driving schedule, for
 156 each vehicle (g). We fit these FE estimates to a curve as a function of the average speed for each
 157 driving schedule, producing a FSC for each vehicle on each facility type (h). Finally, the freeway
 158 and arterial FSC for each vehicle are normalized to the average speeds implied by EPA test
 159 driving schedules (i). Section 5 describes a proposed method for implementation of these
 160 normalized FSC in a long-range scenario analysis tool. We next describe components of the
 161 modeling methodology in more detail.



162

163

Figure 1. Overview of Modeling Methodology to Generate Normalized FSC

164 **3.1 Fuel Consumption Model**

165 Based on an investigation of potential fuel consumption models, the Physical Emissions
166 Rate Estimator (PERE) is selected as the most appropriate model for this research [4]. PERE is a
167 physical vehicle fuel consumption model developed by the EPA to supplement the MOVES
168 mobile-source emissions model for untested vehicles. PERE adopts a physical approach (similar
169 to the well-known Comprehensive Modal Emissions Model [21]) that is ideal for advanced
170 vehicle technologies without vehicle test data. It also utilizes parameters that are aligned with the
171 scope of vehicle-class modeling performed here. PERE models vehicles in less detail than
172 individual vehicle models such as ADVISOR [13] – which is a limitation in some contexts but
173 appropriate for macroscopic scenario analysis where vehicle characteristics are uncertain.

174 The primary vehicle input parameters for PERE (in general order of importance as
175 indicated in the PERE documentation) are:

- 176 1. Vehicle type
- 177 2. Engine indicated (thermal) efficiency
- 178 3. Vehicle model year
- 179 4. Road load power (method and coefficients)
- 180 5. Vehicle weight
- 181 6. Engine size (displacement)
- 182 7. Motor peak power (HEV/EV only)
- 183 8. Fuel cell power rating (FCV only)
- 184 9. Hybrid threshold (HEV only)
- 185 10. Powertrain type (ICE, HEV, EV, FCV)
- 186 11. Fuel type (gas or diesel for ICE – representing spark-ignition or compression-ignition
187 engines)
- 188 12. Transmission type (automatic or manual)

189 The details and model sensitivity for these parameters are discussed in the PERE
190 documentation [4]. In addition to the vehicle parameters, PERE modeling requires an input
191 driving schedule. The driving schedule is a time series of second-by-second vehicle speeds.
192 Vehicle acceleration is differentiated from the speeds, and VSP is calculated using a Road Load
193 Power method, described in the documentation. VSP is a proxy for engine loading, widely used
194 in vehicle emissions and fuel consumption modeling [22], [23].

195 There are two primary caveats of the PERE modeling approach: 1) PERE only models
196 parallel-configuration HEV, not series-configuration, and 2) the application of PERE for EV has
197 not yet been validated. The first is not major concern, since not all possible advanced-vehicle
198 powertrain configurations can be included at this scale of analysis. The second is more of a
199 concern, but a reasonable limitation given the lack of available validation data at the time of
200 development. There are still few data available on the real-world fuel consumption performance
201 of EV, and PERE is considered the best available tool for this study. It lends confidence to the
202 modeling of EV in PERE that EV are modeled as modified HEV (with the ICE removed), and
203 the HEV model in PERE has been well validated [4].

204 3.2 Strategy for Implementing PERE

205 The PERE documentation describes a method for using PERE to derive advanced vehicle
206 fuel consumption rates for MOVES modeling [4]. By this method, the vehicles of interest are
207 modeled over a combination of transient driving schedules, and the average fuel consumption
208 rates binned by the 17 VSP bins used in MOVES [11]. With fuel rates tabulated by VSP bin for
209 each vehicle, total fuel consumption can be quickly computed from the VSP-distribution of
210 second-by-second vehicle activity.

211 Vehicle activity distribution by VSP can be computed from speed profiles – such as
212 embodied in driving schedules [24]. Using coastdown coefficients A, B, and C (also known as
213 Road Load Coefficients - RLC) from the dynamometer load equation, VSP is calculated as
214

$$215 \quad VSP = A \frac{v}{m} + B \frac{v^2}{m} + C \frac{v^3}{m} + 1.1v(a + g * \text{grade}) \quad (1)$$

216
217 from [4], where VSP is in kW/Mg, v is speed in m/s, a is acceleration in m/s^2 , g is the
218 acceleration due to gravity in m/s^2 , and m is vehicle mass in Mg. The three RLC correspond to
219 rolling, rotating, and aerodynamic resistive factors, respectively [4].

220 The RLC, if not provided as a vehicle parameter, can be estimated from the vehicle mass
221 or the Track Road Load HorsePower (TRLHP) [4], [25]. This approach of using many driving
222 schedules to estimate fuel rates by VSP bin then distributing activity by VSP bin provides more
223 fuel consumption data in each VSP bin and more vehicle activity flexibility than simply using a
224 single driving schedule to model fuel rate at an average speed.

225 The adopted strategy for advanced vehicle modeling in this research mirrors the PERE-
226 MOVES approach. The additional benefit of this approach is that vehicle activity distributions by
227 VSP bin can be adjusted based on projected changes in roadway operations, vehicle
228 performance, or driver behavior. In this way fuel-speed curves can be sensitive to changing
229 traffic operations and driving behaviors without repeating the engine/fuel modeling process.

230 3.3 Driving Schedules

231 The EPA has generated facility-specific driving schedules (included in the MOVES
232 model) for different levels of congestion based on real-world measurements. The MOVES
233 driving schedules are designed to reflect actual on-road vehicle activity (in contrast to the
234 standardized dynamometer test schedules), and so represent actual congestion effects [9], [10].
235 The MOVES database includes 18 relevant Light-Duty (LD) driving schedules on freeways and
236 arterials with average speeds from 3 to 76 mph. Concatenating the relevant MOVES driving
237 schedules for modeling in PERE leads to a long (3.7 hour) composite driving schedule for binned
238 fuel rate estimates. As discussed above, it is possible that new engine/powertrain technologies
239 could influence driving patterns for certain speed-facility combinations. Given the uncertainty
240 that this is a real effect – and if it is real, what exactly the effect would be – we use the same
241 driving schedules for all vehicles modeled.

242 In addition to the MOVES driving schedules, we apply real-world vehicle speed data
243 collected on an urban freeway in Portland, Oregon. Vehicle speed data were gathered on OR-217
244 in the summer and fall of 2010 using second-by-second Global Positioning System (GPS) data in
245 a probe vehicle (passenger car). This freeway had average daily traffic of about 100,000 vehicles
246 in 2009 [26], with regular peak-period congestion in both directions. In total, 59 probe vehicle
247 runs of 6.4 miles each were collected before, during, and after the PM peak period. This
248 produced over ten hours of data, with average speeds on each run from 18 to 54 mph. Lastly, fuel
249 economy is also estimated for the set of EPA test driving schedules used for fuel economy
250 labeling [11].

251 **3.4 Vehicle Characteristics**

252 FSC are generated for the following light-duty vehicle types: conventional ICE (spark-
253 ignition and compression-ignition), HEV, EV, and FCV. Vehicle parameter assumptions as
254 required by PERE are based on a variety of sources. Many representative characteristics are
255 included as defaults within the PERE model (transmission shift points, mechanical efficiency,
256 etc.). Other vehicle characteristics are based on the literature – vehicle projection studies and
257 similar research on future vehicle performance [2], [4], [11], [12], [14], [18], [27], [28]. Some
258 vehicle characteristics (such as RLC) are based on EPA inventory data and modeling guidance
259 for the U.S. vehicle fleet [27].

260 Additionally, some vehicles' characteristics are based on manufacturers' specifications.
261 We include in the vehicle test matrix vehicles of known attributes (for the 2010 model year),
262 including:

- 263 • HEV: Toyota Prius, Toyota Camry Hybrid, Toyota Highlander Hybrid, Honda Civic
264 Hybrid, Honda CR-Z Sport Hybrid, Honda Insight, Ford Escape Hybrid, and Ford
265 Fusion Hybrid
- 266 • EV: Nissan Leaf, Tesla Roadster, Coda, and Mitsubishi MiEV
- 267 • FCV: Toyota FCHV, Ford Focus, GM HydroGen3, and Honda FCX

268 Because of the intended use of FSC for long-range scenario analysis with uncertain fleets,
269 the vehicle generation strategy is not to constrain the modeling to existing or even prototype
270 vehicles. The selected vehicle attributes thus include not only the probable but also the possible
271 range of characteristics. In other words, we set the bounds wide enough to capture an uncertain
272 future fleet. Note that in some cases, that means widening the original range of attributes tested
273 in the PERE model (such as for hybrid thresholds).

274 The key parameters varied over vehicles for FSC shape sensitivity testing are:

- 275 1. Vehicle weight
- 276 2. Combustion engine size (displacement)
- 277 3. Engine indicated efficiency (the thermodynamic efficiency limit of the engine)
- 278 4. Electric motor peak power
- 279 5. Fuel cell power rating
- 280 6. Hybrid threshold (the power demand at which the engine or fuel cell is required in
281 addition to the motor in an HEV or FCV)

282 7. Transmission type (automatic or manual)
 283 8. Fuel type (gasoline or diesel – also indicates spark-ignition or compression-ignition)
 284 9. Power accessory load (such as air conditioning)
 285 10. Road Load Coefficients (also used in VSP calculation)
 286 11. Model year (which impacts engine and torque parameters through assumed trends)
 287 Other parameters included in the PERE model are not varied due to low model sensitivity
 288 [4] or no published information on expected changes to the value. Some combustion engine
 289 characteristics are adjusted within PERE based on the vehicle model year (engine friction,
 290 enrichment threshold, peak torque, and peak power). The RLC coefficients for VSP calculation
 291 (see Equation 1) are based on EPA documentation [27] or estimated from the vehicle weight as
 292 described in the PERE documentation [4]. For fuel types other than gasoline or diesel (such as
 293 electricity), PERE converts consumed energy to gasoline equivalent units using an assumed
 294 energy density for gasoline of 32.7 MJ/L.

295 The ranges of tested values of vehicle parameters are:

- 296 • Model year: 2005 to 2040
- 297 • Fuel type: gasoline, diesel
- 298 • Transmission type: manual, automatic
- 299 • Powertrain type: conventional ICE, hybrid, electric, fuel cell
- 300 • Engine size: 1.0 to 4.5 liters
- 301 • Vehicle curb weight: 2,000 to 5,000 lbs
- 302 • Road load method: weight-based and RLC
- 303 • Hybrid threshold: 1 to 6 kW
- 304 • Motor peak power: 10 to 215 kW
- 305 • Fuel cell power rating: 60 to 155 kW
- 306 • Accessory load: 0.75 to 4 kW
- 307 • Engine indicated efficiency: 0.4 to 0.6 gasoline, 0.45 to 0.6 diesel

308
 309 The range of vehicle characteristics is tested over a set of 145 vehicles (not every
 310 possible combination of characteristics is modeled). The vehicles represent a range from very
 311 small neighborhood electric vehicles to large pickup trucks and Sports Utility Vehicles. Note that
 312 these parameters are modeled over their range of values, not simply at the extremes. While the
 313 ranges are wide compared to probable vehicle attributes, they also include the set of expected
 314 vehicles. Space constraints prevent inclusion of the full table of modeled vehicle attributes.
 315 However, vehicles of key interest are included below in Table 1.

316 3.5 Fuel-Speed Curve Calculation

317 The fuel speed curves are calculated from the model output as follows. Let f_b be the
 318 PERE-modeled fuel consumption rate (in kg/second) in VSP bin b , where $b \in B$ and B is the set
 319 of 17 VSP bins. This is (e) in Figure 1. For EV and FCV, note that f_b is presented in gasoline-
 320 equivalent units. Let t_b be the amount of driving time (in seconds) spent in VSP bin b for a given

321 driving schedule – (f) in Figure 1. Then the modeled fuel consumption (in kg) for that driving
 322 schedule is calculated

$$324 \quad f = \sum_{b \in B} (t_b \cdot f_b) . \quad (2)$$

325
 326 For a given fuel density of d_f in kg/gallon and a driving schedule distance of D in miles, the fuel
 327 economy FE (in gasoline-equivalent miles per gallon – mpg) for that driving schedule is then
 328 calculated

$$330 \quad FE = \frac{D \cdot d_f}{f} . \quad (3)$$

331
 332 This is (g) in Figure 1. We use $d_f = 0.744$ kg/L for gasoline and $d_f = 0.811$ kg/L for diesel
 333 from the PERE model, which converts to $d_f = 2.82$ kg/gallon and $d_f = 3.07$ kg/gallon ,
 334 respectively. The average speed for the driving schedule, v , is simply $v = \frac{3600 \cdot D}{\sum_{b \in B} t_b}$. Note that the
 335 driving schedule is indicative of both average speed and speed variability at varying levels of
 336 congestion for typical conditions (see Section 2.1).

337 This fuel modeling approach creates discrete FE–speed data points, so a curve fit is
 338 applied to establish a full FSC – (h) in Figure 1. We fit the FSC to an exponentiated 4th-order
 339 polynomial functional form, following previous emissions modeling research [5], [7], [29]. The
 340 functional form is

$$342 \quad FE = \exp\left(\sum_{i=0}^4 \alpha_i v^i\right) , \quad (4)$$

343
 344 where v is the average travel speed in mph and α_i are fitted parameters. The FSC are fit to this
 345 functional form using an iteratively reweighted least squares method. Separate fits are made for
 346 freeway and arterial driving schedules. Freeway driving schedules include MOVES and OR-217
 347 sources. Arterial driving schedules are sourced from MOVES only.

348 Since average fuel economy is an input to the GreenSTEP model, the FSC are only used
 349 to adjust fuel economy for varying congestion levels (see Section 2.3). Therefore, we need not
 350 calculate absolute fuel economy, but simply how the fuel economy varies with average speed. To
 351 do this, we scale the freeway FSC to the modeled FE at the average speed of the “highway” EPA
 352 test driving schedule (HFET) – 48.2 mph [11]. For arterials we take a similar approach, using a
 353 reference speed 24.4 mph. For FSC normalization to a reference speed v_{ref} , the normalized fuel
 354 economy, FE_{norm} , is calculated

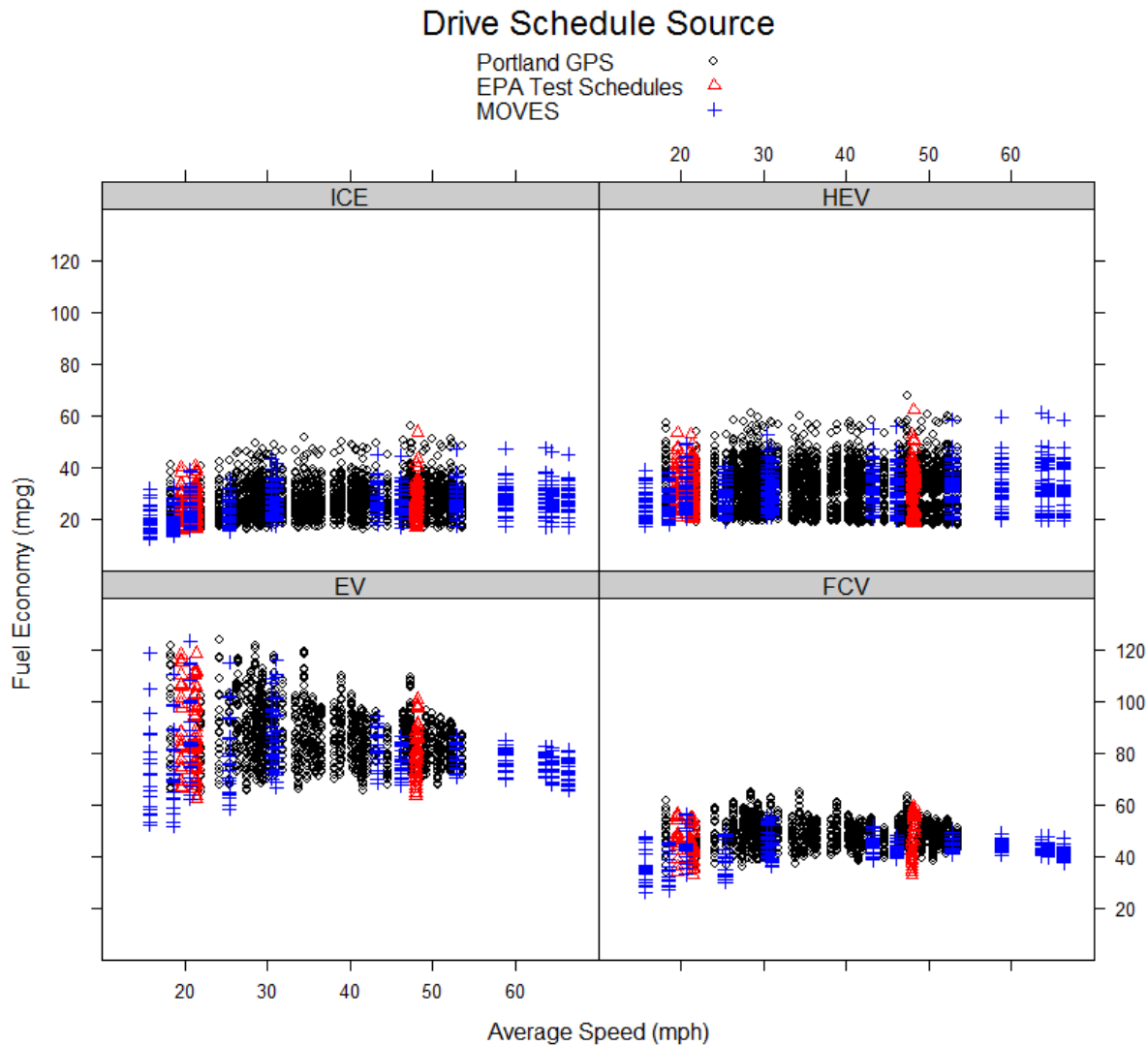
$$355 \quad FE_{norm} = \exp\left(\sum_{i=1}^4 \alpha_i (v^i - v_{ref}^i)\right) . \quad (5)$$

357

358 **4 Results**

359 **4.1 Fuel Economy and Average Speed**

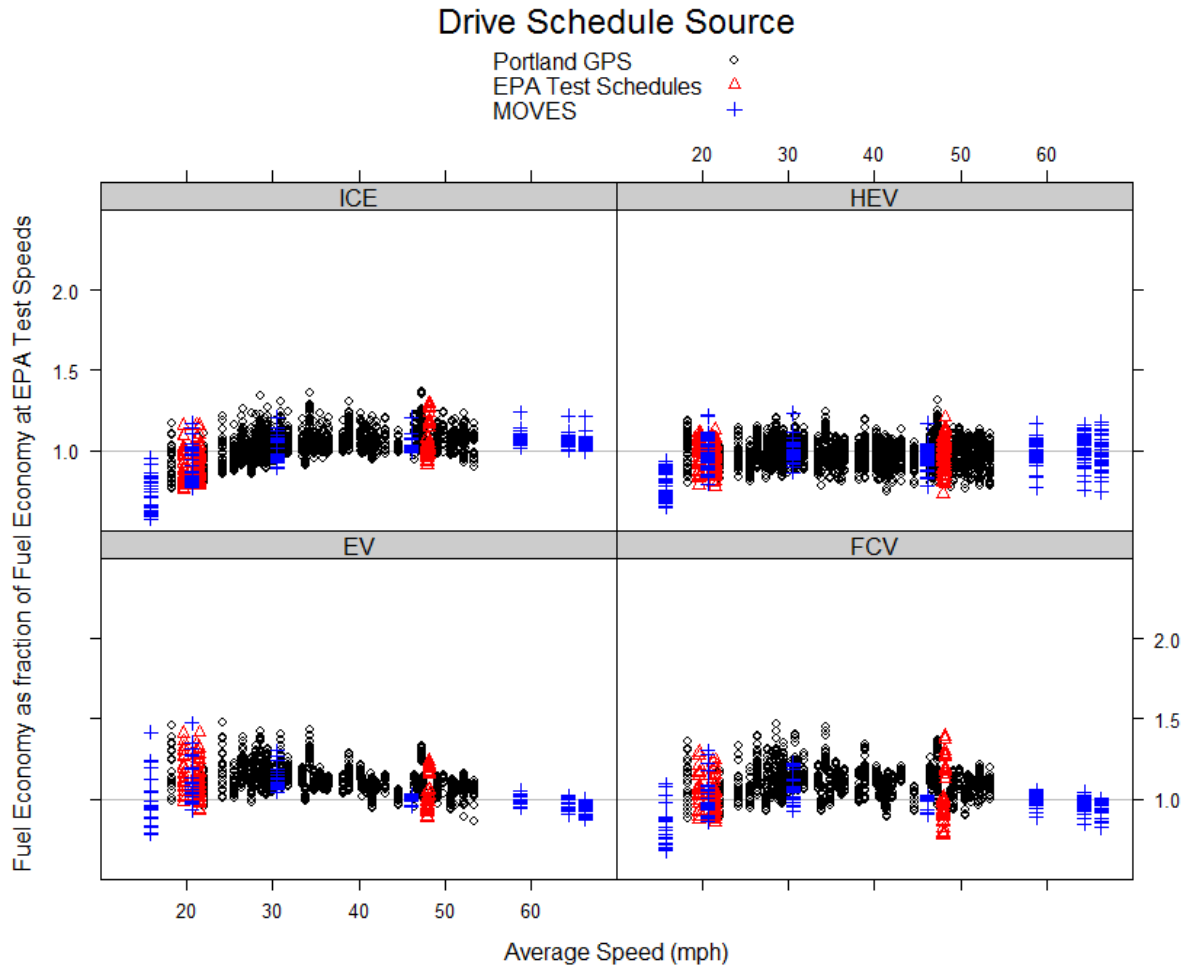
360 Figure 2 shows the FE-speed data points for all vehicles using all driving schedules. The
 361 figure is segmented by powertrain type, with different symbols to represent the different driving
 362 schedule sources and FE in gasoline-equivalent units. From Figure 2, we see that EV have the
 363 highest fuel economy and ICE the lowest. EV also have the widest range of fuel economies for
 364 the modeled vehicles (particularly at lower speeds). For each powertrain type the fuel economy
 365 values are fairly steady across the range of average speeds, with the exception of EV.



366
 367 **Figure 2. Fuel Economy vs. Average Speed by Powertrain Type for All Driving Schedules**

368 Figure 3 presents the same data, but normalized to the freeway reference speed and
 369 excluding MOVES arterial driving schedules. Higher values of normalized FE indicate improved
 370 efficiency with respect to the reference speed conditions. These results are similar to Figure 2,

371 but with some of the inter-vehicle overall fuel economy differences removed – thus illuminating
 372 the impacts of average speed. ICE vehicle FE is generally flat from free-flow speed down to
 373 around 35 mph, at which point FE begins to decrease. For HEV the FE is nearly flat for all
 374 except the lowest-speed MOVES driving schedule. EV fuel economy *increases* with decreasing
 375 speed from free-flow conditions, down to around 20-30 mph. FCV fuel economy also increases
 376 somewhat as speed decreases.

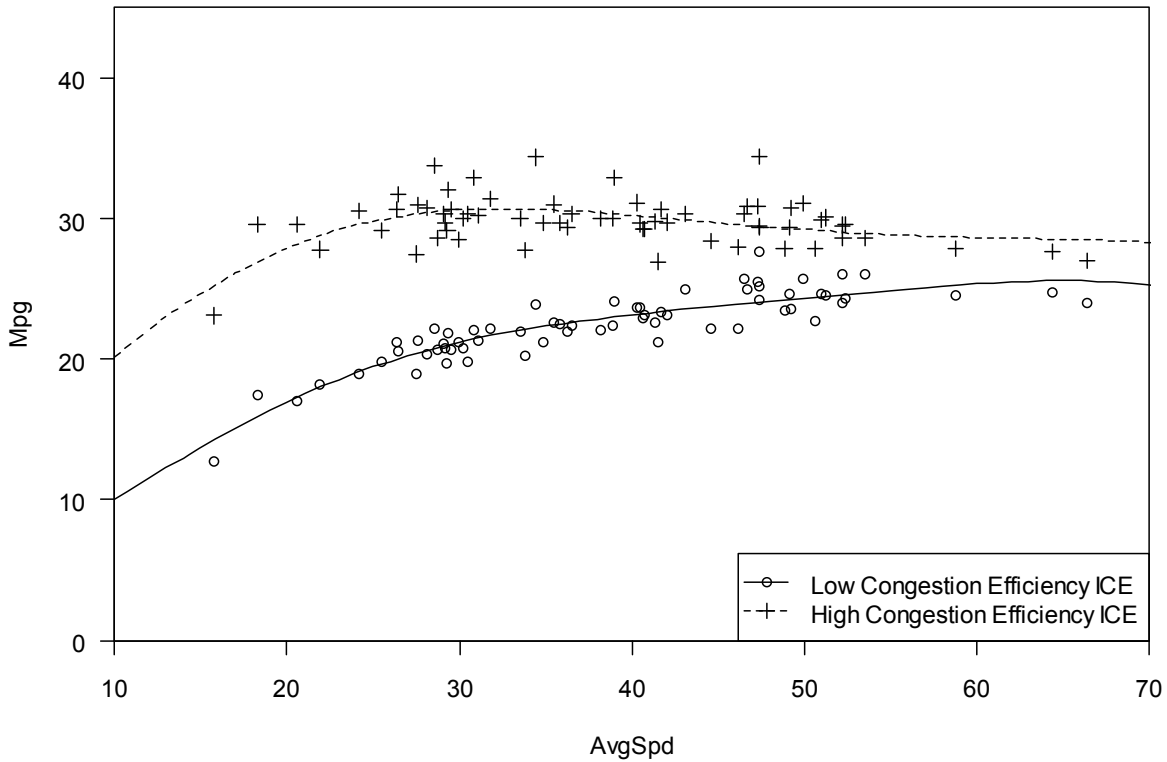


377
 378 **Figure 3. Fuel Economy (Normalized to Reference Speed) vs. Average Speed by Powertrain**
 379 **Type for Freeways**

380 **4.2 Fuel-Speed Curves**

381 This section presents the fitted FSC from Equation 4. Two example fits for freeway FSC
 382 are shown in Figure 4. Here, two fitted FSC are shown along with the base data (using the
 383 MOVES and OR-217 driving schedules). The example low-congestion-efficiency ICE vehicle is
 384 a heavy, high-powered gasoline-fueled passenger car. The fit has an approximate R-squared
 385 value of 0.96 (calculated as Nagelkerke’s generalized R-squared). The example high-congestion-

386 efficiency ICE vehicle is a diesel-fueled passenger truck with moderate power and weight. This
 387 fit has a generalized R-squared value of 0.86.

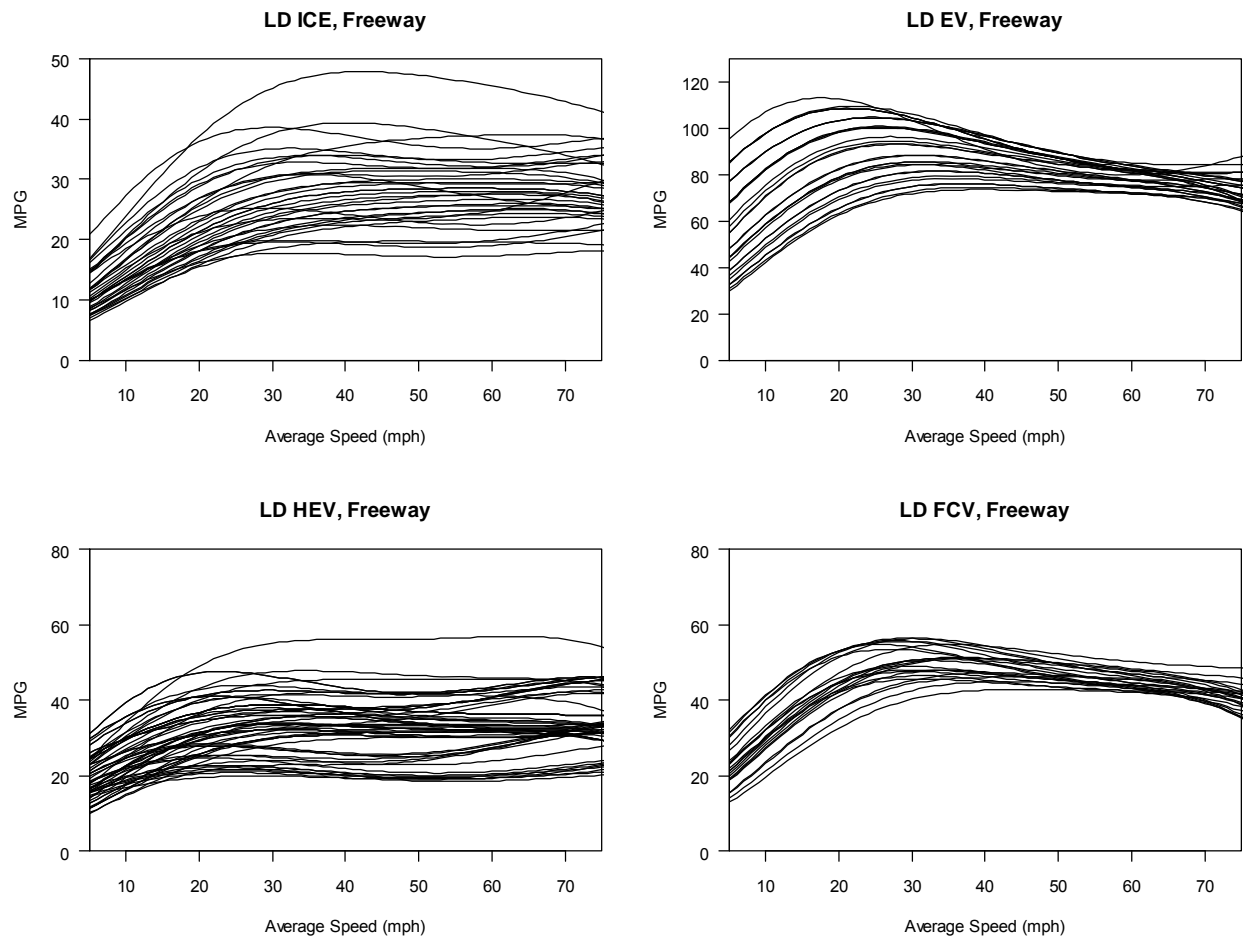


388

389

Figure 4. Example Freeway FSC Fits

390 Figure 5 shows fitted freeway FSC for all modeled vehicles, segmented by powertrain
 391 type (again in gasoline-equivalent mpg). There is a wide variety of FE values and FSC shapes, as
 392 expected from Figure 2 (note the different vertical scales). Generally, ICE vehicles have varying
 393 relationships with speed (positive or negative) for speeds above 30 mph, and decreasing FE at
 394 lower speeds below 30 mph. HEV are less sensitive to congestion, with some vehicles' FE not
 395 decreasing until below 20 mph. Some HEV have about the same FE performance as ICE vehicles
 396 – particularly those with low hybrid thresholds. EV and FCV both show increasing FE with
 397 decreasing speed in Figure 5, down to a speed in the range of 20-40 mph.



398

399

Figure 5. Modeled Individual Freeway FSC by Powertrain Type

400 **4.3 Sensitivity of Fuel Economy in Congestion to Vehicle Characteristics**

401 Fuel economy can vary widely among vehicles for any one driving schedule, as
 402 illustrated in Figure 2. This is due to variability in both fuel rates and VSP distributions of
 403 operating time. In this section we examine how vehicle characteristics influence the Fuel-Speed
 404 data points. Of particular interest is which vehicle characteristics impact the shape of the FSC –
 405 i.e., which characteristics most affect relative vehicle performance in congestion. This is
 406 different from which vehicle characteristics impact overall fuel economy, and sometimes shows
 407 opposite effects. For example, vehicle parameters that mostly improve FE at higher speeds
 408 (decreased drag coefficients, for example) will result in poorer *relative* FE in congestion.

409 Sensitivity analyses show that vehicle weight, engine displacement/fuel cell power, RLC,
 410 hybrid threshold, and accessory load are the vehicle characteristics that have the most impact on
 411 the fuel economy effects of congestion. Higher vehicle weight, engine size, and accessory load
 412 all decrease relative performance in congestion for ICE vehicles, while higher RLC increase
 413 relative performance. Compared to cars, passenger trucks and SUV's tend to have more weight
 414 and engine power (which both reduce performance in congestion), but also higher RLC (which

415 improves *relative* performance in congestion by disproportionately decreasing efficiency at high
416 speeds). Higher motor peak power slightly increases relative congestion performance for EV, but
417 higher fuel cell power rating decreases relative congestion performance for FCV.

418 HEV performance in congestion increases with hybrid threshold (since more low-power
419 driving is powered by recovered energy). For HEV the motor and battery characteristics
420 combined with the driving patterns will determine the true hybrid threshold. Assuming HEV
421 improve over time to allow higher hybrid thresholds, the relative HEV performance in
422 congestion will improve as well. Unlike ICE vehicles, HEV can improve their relative FE in
423 congestion with larger engine sizes, because they can utilize the larger ICE nearer optimum
424 efficiency for high power loads but turn off the combustion engine during low-power driving
425 events in congestion. In this study, motor peak power was not a limiting factor in relative
426 efficiency for HEV. High accessory power loads notably degrade the relative efficiency in
427 congestion for fuel efficient vehicles, since a greater portion of total energy demand in
428 congestion is from the static accessory load. Since much of the expected accessory load is from
429 air conditioning usage, improvements over time such as advanced window glazings and cabin
430 ventilation [28] can increase the relative FE in congestion for advanced vehicles.

431 Power demands vary due to external vehicle forces only (mass and RLC inputs), while
432 fuel rates are influenced by all vehicle attributes. From Equation 1, the RLC and vehicle mass
433 have larger impacts at higher speeds (the impact of RLC “*C*” increases with the cube of speed).
434 The impact of acceleration, however, is independent of mass or RLC. Thus, the VSP distribution
435 of high-speed freeway driving schedules (with higher speeds and fewer accelerations) is more
436 impacted by vehicle characteristics (mass and RLC) than the VSP distribution of arterial driving
437 schedules (with more accelerations and lower speeds). More generally, the VSP distribution of
438 vehicle activity in uncongested driving conditions is more impacted by vehicle characteristics
439 than in congested driving conditions. The same holds for arterial versus freeway driving, with
440 freeway driving more impacted by vehicle characteristics.

441 As demonstrated in Figure 5, there is a range of potential FSC shapes for each vehicle
442 type, depending on the specific vehicle characteristics. Projecting this array of characteristics for
443 future vehicle fleets in scenario analysis is impractical. The next section describes a suggested
444 approach for incorporating these FSC into scenario analysis.

445 **5 Applying Fuel-Speed Curves for Scenario Analysis**

446 This section describes a recommended method for applying advanced-vehicle FSC for
447 scenario analysis, considering the range of plausible curve shapes shown in Section 4. The
448 recommended approach is to use minimum/maximum sensitivity normalized FSC as the bounds
449 of congestion effects. Interpolating between these extreme curves provides speed-based FE
450 adjustment factors to calculate congestion effects on overall fuel economy.

451 The interpolation distance between the bound FSC is based on a new model input,
452 “Congestion Efficiency”, which describes the projected performance of each vehicle type in
453 congestion, with respect to “extreme case” vehicles. Congestion Efficiency ranges from 0 for

454 poorest performance to 1 for maximum relative efficiency performance. Using Congestion
 455 Efficiency CE and upper and lower bound *normalized* FSC with curve fit parameters $\alpha_{U,i}$ and
 456 $\alpha_{L,i}$, respectively, the interpolated normalized FSC curve is calculated

$$457 \quad FE = CE \cdot \exp\left(\sum_{i=0}^4 \alpha_{U,i} v^i\right) + (1 - CE) \exp\left(\sum_{i=0}^4 \alpha_{L,i} v^i\right) . \quad (6)$$

459
 460 The determination of CE in scenario analysis is based on the sensitivities described in Section
 461 4.3. This approach avoids introducing numerous new vehicle parameters to the scenario analysis,
 462 while still allowing some assumptions about the future vehicle fleet to inform the congestion
 463 adjustment values.

464 We selected extreme-case vehicles for FSC bounds based on comparison of the FSC
 465 shapes and vehicle attributes. Those vehicles selected are the modeled vehicles of each vehicle
 466 type with the highest and lowest relative FE in heavy congestion as compared to FE at free-flow
 467 speed (for each facility type). The vehicle characteristics and FSC fit parameters for the selected
 468 vehicles are shown in Table 1. The corresponding upper-bound and lower-bound FSC are shown
 469 in Figure 6. The selected bounding vehicles in Table 1 are not the most extreme combinations of
 470 attributes possible. Rather, they are modeled mixes of vehicle attributes considered possible (if
 471 not probable) based on the literature.

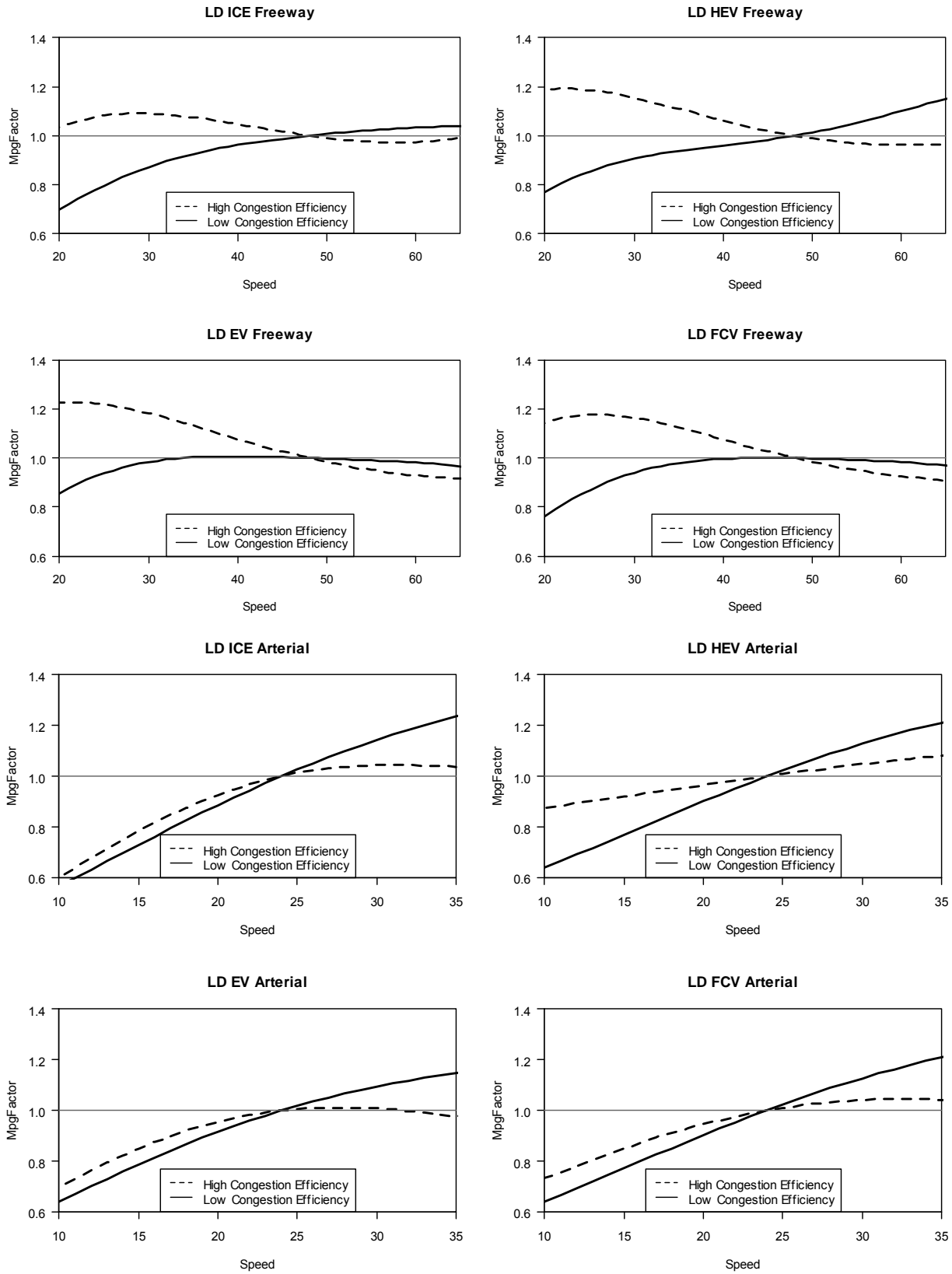
472 **Table 1. Extreme-Case Vehicles: Characteristics and FSC Fit Parameters**

Congestion Efficiency	Freeways							
	ICE*		HEV*		EV**		FCV**	
	Low	High	Low	High	Low	High	Low	High
Passenger Car/Truck	Car	Truck	Car	Car	Car	Car	Car	Car
Curb Weight (lbs)	5,000	2,500	2,504	2,000	3,800	2,000	3,000	2,000
Engine Displ. (L)	4.5	2.0	1.1	2.0	NA	NA	NA	NA
RLC: A	156.46	235.01	156.46	156.46	156.46	156.46	156.46	156.46
RLC: B	2.002	3.039	2.002	2.002	2.002	2.002	2.002	2.002
RLC: C	0.493	0.748	0.493	0.493	0.493	0.493	0.493	0.493
Motor Peak Power/ Fuel Cell Rating (kW)	NA	NA	68	10	80	100	140	40
Hybrid Threshold (kW)	NA	NA	2	4	NA	NA	NA	NA
Accessory Power (kW)	0.75	0.75	4	0.75	4	0.75	4	0.75
Total Peak Power (kW)	220	98	123	108	80	100	140	40
Specific Power (W/kg)	97	86	108	119	46	110	103	44
α_0	1.514	2.331	1.892	3.122	2.911	4.236	1.984	3.048
α_1	0.1112	0.0809	0.1321	0.0667	0.1132	0.0511	0.1324	0.0955
α_2	-0.0029	-0.0025	-0.0041	-0.0025	-0.0034	-0.0019	-0.0037	-0.0032
α_3	3.63E-5	2.94E-5	5.78E-5	3.44E-5	4.55E-5	2.41E-5	4.60E-5	4.27E-5
α_4	-1.73E-7	-1.15E-7	-2.90E-7	-1.63E-7	-2.27E-7	-1.04E-7	-2.18E-7	-2.00E-7

Congestion Efficiency	Arterial							
	ICE*		HEV*		EV**		FCV**	
	Low	High	Low	High	Low	High	Low	High
Passenger Car/Truck	Car	Truck	Car	Car	Car	Car	Car	Car
Curb Weight (lbs)	3,750	2,500	3,000	3,020	3,800	2,000	3,000	2,000
Engine Displ. (L)	4.5	2.0	1.8	1.3	NA	NA	NA	NA
RLC: A	156.46	235.01	156.46	154.69	156.46	156.46	156.46	156.46
RLC: B	2.002	3.039	2.002	1.977	2.002	2.002	2.002	2.002
RLC: C	0.493	0.748	0.493	0.487	0.493	0.493	0.493	0.493
Motor Peak Power/ Fuel Cell Rating (kW)	NA	NA	60	10	80	100	140	40
Hybrid Threshold (kW)	NA	NA	2	2	NA	NA	NA	NA
Accessory Power (kW)	4	0.75	4	0.75	4	0.75	4	0.75
Total Peak Power (kW)	220	98	148	76	80	100	140	40
Specific Power (W/kg)	129	86	109	55	46	110	103	44
α_0	1.392	2.331	1.803	2.71	2.911	4.236	1.984	3.048
α_1	0.1145	0.0809	0.1204	0.0765	0.1132	0.0511	0.1324	0.0955
α_2	-0.0029	-0.0025	-0.0034	-0.0031	-0.0034	-0.0019	-0.0037	-0.0032
α_3	3.45E-5	2.94E-5	4.36E-5	4.77E-5	4.55E-5	2.41E-5	4.60E-5	4.27E-5
α_4	-1.55E-7	-1.15E-7	-2.06E-7	-2.42E-7	-2.27E-7	-1.04E-7	-2.18E-7	-2.00E-7

* Gasoline-fueled, automatic transmission, engine indicated efficiency of 0.4, model year 2010

** EV and FCV are the same vehicles for arterials and freeways, model year 2010



473

474

475

Figure 6. Upper and Lower Bound Normalized FSC

476 Table 2 lists the vehicle characteristics that are expected to impact the relative efficiency
 477 in congestion (*CE*) for each vehicle powertrain type. This table is based on sensitivity analysis of
 478 the modeled vehicle attributes and FSC. Qualitative projection of these attributes can be used to
 479 set the new model input, Congestion Efficiency, between 0 and 1. The median Congestion
 480 Efficiency value is 0.5, which puts the FE adjustment curve midway between the extreme curves
 481 shown in Figure 6. If we expect, for example, average HEV to get lighter over time, we can set
 482 the Congestion Efficiency to trend upward for future model years. Note again that *CE* is
 483 increased both by attributes that improve FE in congestion and by attributes that
 484 disproportionately decrease FE at higher speeds.

485 **Table 2. Vehicle Characteristics Influencing Relative Congestion Efficiency**

Powertrain type	Low Relative Congestion Efficiency	High Relative Congestion Efficiency
ICE	heavier weight, larger engine, lower RLC, gasoline fuel, higher accessory loads, earlier model year	lighter weight, smaller engine, higher RLC, diesel fuel, lower accessory loads, later model year
HEV	heavier weight, smaller ICE, lower RLC, lower hybrid threshold, gasoline fuel, higher accessory loads, earlier model year	lighter weight, larger ICE, higher RLC, higher hybrid threshold, diesel fuel, lower accessory loads, later model year
EV	heavier weight, lower RLC, higher accessory loads	lighter weight, higher RLC, lower accessory loads
FCV	heavier weight, higher fuel cell power rating, lower RLC, higher accessory loads	lighter weight, lower fuel cell power rating, higher RLC, lower accessory loads

486
 487 As a final consideration, we examine the potential impacts of these FSC on overall FE.
 488 Using a Congestion Efficiency of 0.5, at 25 mph the freeway ICE FE adjustment factor is 0.94
 489 and all three advanced powertrain vehicle types have FE adjustments over 1 (i.e. efficiency
 490 benefits). On arterials, the minimum adjustment factor at 20 mph (for ICE) is 0.92. Thus, the
 491 potential adjustments to FE for typical congestion are small. With evolving vehicle fleets
 492 containing more advanced vehicles, it is unlikely that the net effect of congestion on FE will be
 493 substantially detrimental – and the net effect could be beneficial.

494 6 Conclusions

495 This paper describes research undertaken to establish plausible fuel-speed curves (FSC)
 496 for advanced vehicles, to be used in long-term transportation scenario analysis. We use the PERE
 497 fuel consumption model with real-world driving schedules and a range of advanced vehicle
 498 characteristics to estimate vehicle fuel economy in varying traffic conditions. The fuel-speed
 499 data points are then used to generate normalized fuel economy versus average speed curves for
 500 each of 145 modeled vehicles.

501 Analysis of the FSC shows that advanced powertrain vehicles are expected to perform
 502 better in congestion than ICE vehicles (with respect to FE at free-flow speeds). Many ICE
 503 vehicles do not lose fuel efficiency until traffic slows to about 30 mph. HEV are less sensitive to

504 average speed changes than ICE vehicles, and tend to maintain their fuel efficiency down to 20
505 mph, due to recaptured braking energy. Fuel efficiency *increases* for EV down to about 20-30
506 mph, below which it degrades. FCV have similar FE effects to EV, though with less sensitivity
507 to speed.

508 Besides powertrain type, congestion effects vary with other vehicle characteristics as
509 well. Relative fuel efficiency at lower speeds improves for vehicles with lighter weight, smaller
510 engines, higher hybrid thresholds, and lower accessory loads (such as air conditioning). *Relative*
511 performance in congestion can also improve with attributes that disproportionately decrease FE
512 at higher speeds, such as higher aerodynamic drag and rolling resistance factors.

513 Considering the normalized FSC sensitivity to multiple attributes, we propose a bounded
514 approach for applying the modeled FSC in scenario analysis. In the proposed method, FE
515 adjustments are an interpolation between extreme-case FSC, based on projection of relative
516 congestion efficiency. This allows adjustment for vehicle trends over time without requiring
517 specificity in the vehicle fleet characteristics.

518 In conclusion, the modeled FSC show that advanced powertrain vehicles can reduce or
519 reverse the fuel efficiency losses associated with typical roadway congestion. On the other hand,
520 advanced vehicles with certain characteristics (heavy and with high accessory power loads, for
521 example) can still have poor relative performance in congestion. The results of this research can
522 assist with broader analysis of the role these differences will play in total fuel consumption and
523 emissions from roadway travel.

524 **References**

- 525 [1] D. Schrank, T. Lomax, and B. Eisele, "Urban Mobility Report 2011," Texas Transportation
526 Institute, College Station, TX, Sep. 2011.
- 527 [2] S. E. Plotkin and M. K. Singh, "Multi-Path Transportation Futures Study: Vehicle
528 Characterization and Scenario Analyses," Argonne National Laboratory (ANL), 2009.
- 529 [3] B. Gregor, "Greenhouse Gas Statewide Transportation Emissions Planning Model
530 (GreenSTEP Model) Documentation - Draft." Oregon Department of Transportation, Nov-
531 2010.
- 532 [4] E. Nam and R. Giannelli, "Fuel Consumption Modeling of Conventional and Advanced
533 Technology Vehicles in the Physical Emission Rate Estimator (PERE)," U.S.
534 Environmental Protection Agency, Draft EPA420-P-05-001, Feb. 2005.
- 535 [5] M. Barth and K. Boriboonsomsin, "Real-World Carbon Dioxide Impacts of Traffic
536 Congestion," *Transportation Research Record: Journal of the Transportation Research*
537 *Board*, vol. 2058, pp. 163–171, 2008.
- 538 [6] M. Barth, G. Scora, and T. Younglove, "Estimating emissions and fuel consumption for
539 different levels of freeway congestion," *Transportation Research Record: Journal of the*
540 *Transportation Research Board*, vol. 1664, pp. 47–57, 1999.
- 541 [7] A. Bigazzi and M. Figliozzi, "An Analysis of the Relative Efficiency of Freeway
542 Congestion Mitigation as an Emissions Reduction Strategy," in *90th Annual Meeting of the*
543 *Transportation Research Board*, Washington, D.C., 2011.

- 544 [8] T. Barlow and P. Boulter, "Emissions factors 2009: Report 2 - a review of the average-
545 speed approach for estimating hot exhaust emissions," UK Department for Transport,
546 Research report PPR355, Jun. 2009.
- 547 [9] R. Smit, A. L. Brown, and Y. C. Chan, "Do air pollution emissions and fuel consumption
548 models for roadways include the effects of congestion in the roadway traffic flow?,"
549 *Environmental Modelling and Software*, vol. 23, no. 10-11, pp. 1262-1270, 2008.
- 550 [10] U.S. Environmental Protection Agency, "Motor Vehicle Emission Simulator (MOVES)
551 2010 User's Guide," Washington, D.C., EPA-420-B-09-041, Dec. 2009.
- 552 [11] U.S. Environmental Protection Agency, "Final Technical Support Document: Fuel
553 Economy Labeling of Motor Vehicle Revisions to Improve Calculation of Fuel Economy
554 Estimates," Washington, D.C., EPA420-R-06-017, Dec. 2006.
- 555 [12] S. C. Davis, S. W. Diegel, and R. G. Boundy, "Transportation Energy Data Book: Edition
556 29," Oak Ridge National Laboratory, Oak Ridge, TN, ORNL-6985, Jul. 2010.
- 557 [13] T. Markel et al., "ADVISOR: a systems analysis tool for advanced vehicle modeling,"
558 *Journal of Power Sources*, vol. 110, no. 2, pp. 255-266, Aug. 2002.
- 559 [14] M. Singh, A. Vyas, and E. Steiner, "VISION Model: Description of Model Used to
560 Estimate the Impact of Highway Vehicle Technologies and Fuels on Energy Use and
561 Carbon Emissions to 2050," Argonne National Laboratory, ANL/ESD/04-1, Dec. 2003.
- 562 [15] M. Earleywine, J. Gonder, T. Markel, and M. Thornton, "Simulated fuel economy and
563 performance of advanced hybrid electric and plug-in hybrid electric vehicles using in-use
564 travel profiles," in *Vehicle Power and Propulsion Conference (VPPC), 2010 IEEE*, 2010,
565 pp. 1-6.
- 566 [16] C. Samaras and K. Meisterling, "Life Cycle Assessment of Greenhouse Gas Emissions
567 from Plug-in Hybrid Vehicles: Implications for Policy," *Environmental Science &
568 Technology*, vol. 42, no. 9, pp. 3170-3176, May 2008.
- 569 [17] C. Silva, M. Ross, and T. Farias, "Evaluation of energy consumption, emissions and cost of
570 plug-in hybrid vehicles," *Energy Conversion and Management*, vol. 50, no. 7, pp. 1635-
571 1643, Jul. 2009.
- 572 [18] A. Delorme, D. Karbowski, and P. Sharer, "Evaluation of fuel consumption potential of
573 medium and heavy duty vehicles through modeling and simulation," Argonne National
574 Laboratory (ANL), 2010.
- 575 [19] G. Fontaras, P. Pistikopoulos, and Z. Samaras, "Experimental evaluation of hybrid vehicle
576 fuel economy and pollutant emissions over real-world simulation driving cycles,"
577 *Atmospheric Environment*, vol. 42, no. 18, pp. 4023-4035, Jun. 2008.
- 578 [20] A. Alessandrini and F. Orecchini, "A driving cycle for electrically-driven vehicles in
579 Rome," *Proceedings of the Institution of Mechanical Engineers, Part D: Journal of
580 Automobile Engineering*, vol. 217, no. 9, pp. 781-789, Jan. 2003.
- 581 [21] M. Barth et al., "Development of a Modal-Emissions Model," Transportation Research
582 Board, Project 25-11, Apr. 2000.
- 583 [22] H. C. Frey, A. Unal, J. Chen, S. Li, and C. Xuan, "Methodology for Developing Modal
584 Emission Rates for EPA's Multi-Scale Motor Vehicle & Equipment Emission System,"
585 U.S. Environmental Protection Agency, Ann Arbor, Michigan, EPA420-R-02-027, Aug.
586 2002.
- 587 [23] G. Song and L. Yu, "Estimation of Fuel Efficiency of Road Traffic by Characterization of
588 Vehicle-Specific Power and Speed Based on Floating Car Data," *Transportation Research*

